

Apparent slip flows in hydrophilic and hydrophobic microchannels

Chang-Hwan Choi, K. Johan A. Westin, and Kenneth S. Breuer^{a)}

Division of Engineering, Brown University, Providence, Rhode Island 02912

(Received 9 April 2003; accepted 7 July 2003; published 2 September 2003)

The slip effects of water flow in hydrophilic and hydrophobic microchannels of 1 and 2 μm depth are examined experimentally. High-precision microchannels were treated chemically to enhance their hydrophilic and hydrophobic properties. The flow rates of pure water at various applied pressure differences for each surface condition were measured using a high-precision flow metering system and compared to a theoretical model that allows for a slip velocity at the solid surface. The slip length was found to vary approximately linearly with the shear rate with values of approximately 30 nm for the flow of water over hydrophobic surfaces at a shear rate of 10^5 s^{-1} . The existence of slip over the hydrophilic surface remains uncertain, due to the sensitivity of the current analysis to nanometer uncertainties in the channel height. © 2003 American Institute of Physics. [DOI: 10.1063/1.1605425]

I. INTRODUCTION

For the past century, the no-slip boundary condition has been assumed to be appropriate for most macroscopic flows. However, it has received new attention recently as engineering applications reach down to the micrometer and nanometer scale, and as diagnostic techniques improve our ability to probe the physics of fluid–surface interactions at the molecular scale. In particular, changes in fluid–surface interactions, such as the wetting ability of the fluid, may affect the ability of the fluid to exchange momentum with the surface at the atomic scale, resulting in a velocity slip at the solid wall.

Slip velocities on both hydrophilic and hydrophobic surfaces have been studied previously using a variety of experimental techniques^{1–7} and have reported slip lengths that vary from about 20 nm⁸ to as high as 1 μm .^{5,7} The wide range slip lengths inferred by these studies, the uncertainty about the dependence on shear rate, as well as the rather limited range of shear rates covered in any single experiment, motivated the current experiment in which slip velocities are carefully measured over a wide range of shear rates and in carefully controlled precision geometries. The current technique correlates the applied pressure gradient with the flow rate of water through a microchannel with carefully controlled geometry and atomically smooth surfaces treated to be either hydrophilic or hydrophobic. The measured data are correlated to the slip length through simple theory based on a quasicontinuum description of the system. These experiments are closely related to experiments by Arkilic, Schmidt, and Breuer, who measured slip velocities⁹ and momentum accommodation coefficients¹⁰ for *gases* flowing through precision-fabricated silicon microchannels. In such cases, gas rarefaction due to the small channel dimension results in slip velocities at the solid surface. The current results continue this work, extending it to liquid flows (which requires a new

flow measuring technique) and also studying the effects of hydrophilic and hydrophobic surface characteristics.

II. EXPERIMENTAL APPROACH

We assume an incompressible fluid flowing through a high aspect ratio channel of height, $2h$, width, w , and length, L , characterized by an unknown slip velocity, u_{slip} , at the solid boundary. The Navier–Stokes equations can be solved for such conditions, yielding the flow rate, Q , as a function of the applied pressure drop, Δp , and the channel geometry:

$$Q = \underbrace{\frac{2wh^3}{3\mu} \frac{\Delta p}{L}}_{Q_{\text{Poiseuille}}} + \underbrace{2hw \cdot u_{\text{slip}}}_{Q_{\text{slip}}} \quad (1)$$

where μ is the fluid viscosity. If all the geometric and fluid parameters are known, u_{slip} can be computed from $Q(\Delta p)$ measurements. By using the Navier hypothesis for fluid slip—that the velocity at a solid surface is proportional to the shear stress at the surface—the slip length, δ , can be computed:

$$\delta = \frac{u_{\text{slip}}}{\dot{\gamma}} = \frac{\mu QL}{2\Delta p wh^2} - \frac{h}{3}. \quad (2)$$

Fabrication processes were chosen to provide good control of the channel height and to obtain atomically smooth surfaces. 0.5 μm of thermal silicon dioxide was grown on double-side-polished *N*-type silicon wafers by wet oxidation. A polysilicon layer of either 0.5 μm or 1.5 μm was deposited by low pressure chemical vapor deposition, serving to both define the channel height of 1 or 2 μm , and later as an intermediate layer for the anodic bonding to a Pyrex wafer.¹¹ The channel geometry was etched into the polysilicon and the oxide layer by reactive ion etching (RIE) and buffered oxide etch (BOE), respectively, and photoresist was used as an etch mask. Then, the inlet–outlet ports (1 mm square) were etched from the backside of the wafer using drop reactive ion etching (DRIE) and a thick photoresist etch mask.

^{a)} Author to whom correspondence should be addressed. Electronic mail: kbreuer@brown.edu

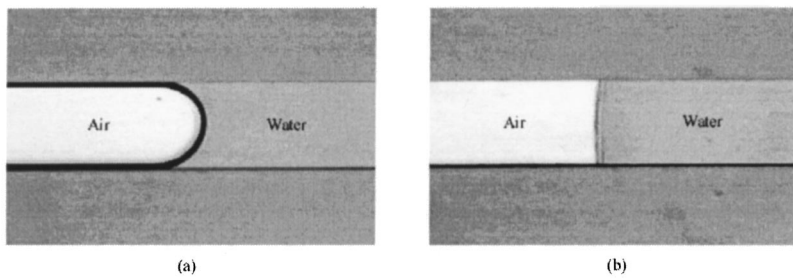


FIG. 1. Meniscus shape of evaporating water inside 21 μm deep and 100 μm wide channel. (a) RCA-1 cleaned hydrophilic channel. (b) OTS-coated hydrophobic channel.

The wafers were then RCA-cleaned and anodically bonded to a polished Pyrex wafer^{12,13} which provides visual access to the channel. The polished surfaces of the Pyrex wafer and the original silicon substrate serve as smooth walls for the channels, with root-mean square (rms) roughness levels measured using atomic force microscopy (AFM) to be less than 11 \AA (3.3 \AA after the hydrophobic coating). All the channels are 500 μm wide and 9 mm long.

The volumetric flow measurements were made using a technique for high-precision volumetric flow measurements developed in our group¹⁴ in which the working fluid (ultra-pure water) is forced through the channel using nitrogen, while the rate of the falling free surface in a precision-bore hole is measured (using a laser distance meter) to determine the flow rate. The system has been tested extensively and demonstrated to have a resolution of 0.1 nl/s.

The channels were tested with both hydrophilic and hydrophobic surface conditions. After the RCA cleaning and anodic bonding steps in the end microfabrication processes, the channel surface should be hydrophilic due to the presence of a thin (0.6–2.0 nm) native oxide layer that spontaneously grows on silicon surfaces.¹⁵ However, to make the channel surfaces more hydrophilic and clean, RCA-1 cleaning was performed prior to each flow rate measurement experiment. RCA-1 solution ($\text{H}_2\text{O} + \text{H}_2\text{O}_2 + \text{NH}_4\text{OH}$, 5:1:1 by volume) was flowed through the channel at 75 $^\circ\text{C}$ for 10 min using a specialized stainless steel fixture. Following this, the system was rinsed by flowing pure deionized (DI) water and finally dried by flowing nitrogen gas. Flow rate data were taken over a range of operating pressures, typically ranging from 0.1 to 1 MPa.

After the flow rate measurements in the hydrophilic case, the same channel was coated with a self-assembled monolayer (SAM) of octadecyltrichlorosilane [$\text{CH}_3(\text{CH}_2)_{17}\text{SiCl}_3$, OTS], making the surface highly hydrophobic.^{16,17} The coating was applied by flowing 5 mM OTS solution in hexadecane through the channel held in a Teflon fixture at 24 $^\circ\text{C}$ for 2 h.^{18,19} Following this, it was rinsed several times by flowing hexane followed by methanol and finally dried by flowing nitrogen gas. The preparation of the OTS solution and all the coating processes were done in a glovebox continuously supplied with dry nitrogen gas to avoid the bulk polymerization which can occur in the presence of water. Finally, the channel was baked at approximately 100 $^\circ\text{C}$ on a hot plate in air for a few hours. The channel was inspected (through the Pyrex window), and a second series of flow rate measurements were then performed. The measurements were repeated in four channels—

two with $h \approx 0.5 \mu\text{m}$ and two with $h \approx 1 \mu\text{m}$.

The surface wetting properties can usually be characterized by measuring the water contact angle. However, the water contact angle inside the channel cannot be measured since it is sealed. Instead, the meniscus shape of water evaporating in the channel was monitored to confirm the hydrophobicity of the surface and to ensure that there are no particulates contaminating the surface. As an example of this, Fig. 1 shows the meniscus shape of water evaporating in a 21 μm deep channel with the hydrophilic and hydrophobic surface conditions, respectively. This visually characterizes the wetting property of the surfaces.

III. RESULTS AND DISCUSSION

Typical flow data are shown in Fig. 2 for the case of water in the $h = 0.5 \mu\text{m}$ channel. Note that the flow rates measured in the hydrophobic channel consistently lie above those measured in the same channel, but with a hydrophilic surface condition.

The raw experimental data (flow rate and applied pressure) were reduced to reveal the apparent slip velocity and slip length as functions of shear rate using (1) and (2). Two functional relationships were assumed for the slip length as a function of the shear rate—one governing flow over a hydrophilic surface [$\delta = f(\dot{\gamma})$] and a second governing flow over the hydrophobic surface [$\delta = g(\dot{\gamma})$]. A global optimization procedure was used to determine both these functions simul-

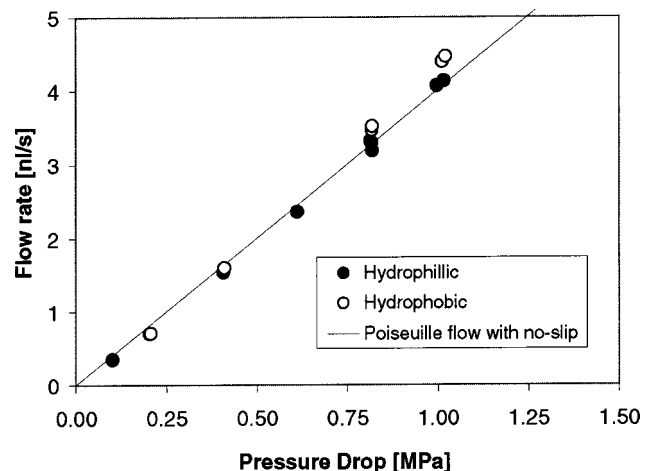


FIG. 2. Flow rate versus applied pressure for pure DI water in the $h = 0.5 \mu\text{m}$ channel. The filled circles are measurements from the channel with a hydrophilic surface condition while the open circles are measurements with the hydrophobic surface condition (in the same channel).

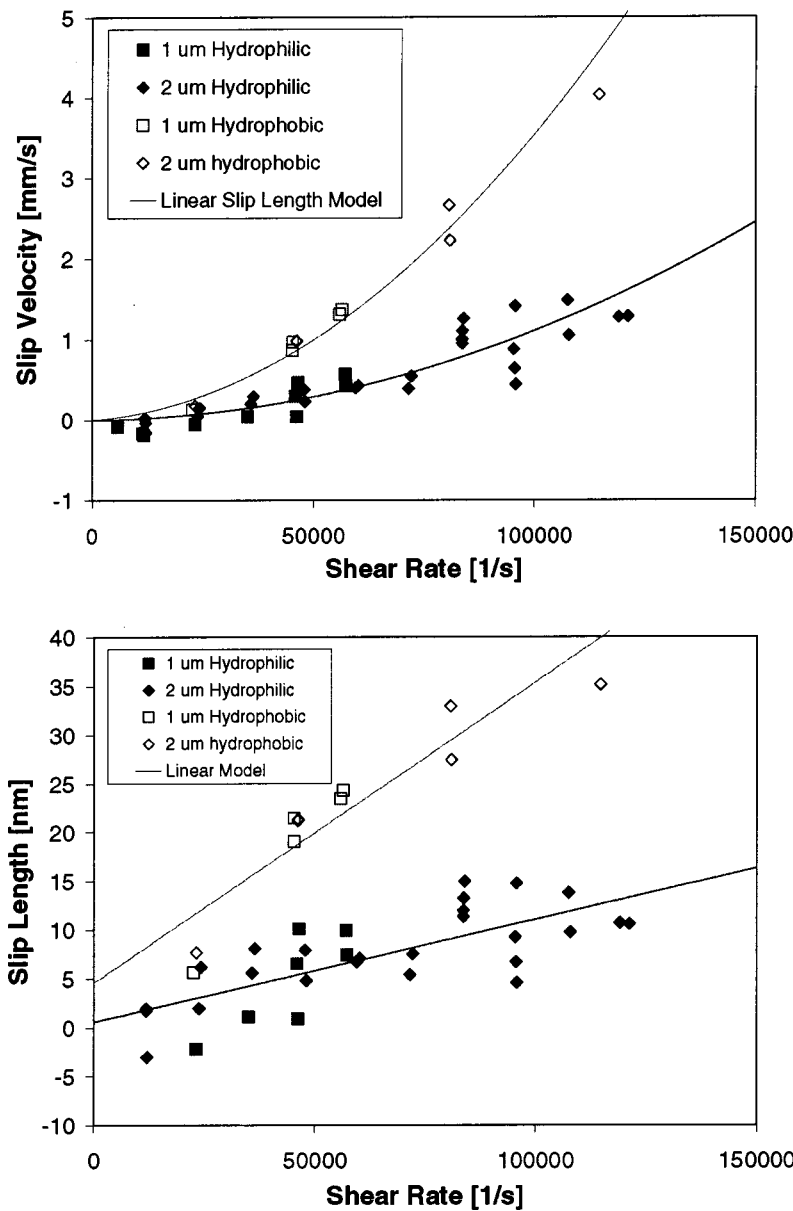


FIG. 3. Slip velocity and associated slip length for pure DI water versus rate of shear. The data analysis allows for slip over both the hydrophilic and hydrophobic surfaces. The slip length dependence is given by $\delta=0.6 + 1.1 \times 10^{-4} \dot{\gamma}$ (for the hydrophilic surface) and $\delta=4.5 + 3.1 \times 10^{-4} \dot{\gamma}$ (for the hydrophobic surface).

taneously, fitting the data from all four channels taken over both the hydrophilic and hydrophobic surfaces (the channel half-height was reduced by 2.3 nm in fitting the hydrophobic experiments, to account for the OTS layer thickness). Although the channel half-height, h , and length of each channel were measured prior to wafer bonding, there are nevertheless some geometric uncertainties due to measurement limits and the growth of oxide layers during bonding and subsequent exposure to the air and the RCA-1 cleaning solution. For this reason, the data analysis technique allowed the value of h for each channel to vary slightly from its prebonding measured value. Such small adjustments were found to significantly improve the collapse of the data. However, the implications of these adjustments will be discussed shortly.

Based on a preliminary inspection of the data, we initially assumed that the slip length depends linearly on the shear rate: $\delta=A+B\dot{\gamma}$, and so the optimization procedure required finding values of A and B for the hydrophilic and hydrophobic surfaces, plus values of h_i for each of the four

channels tested—a total of eight parameters. These parameters were determined from the entire experimental data set—over 100 $\{Q, \Delta p\}$ measurement pairs by minimizing the mean square error between the measured and predicted values of the slip length. The results of this data analysis are shown in Fig. 3 and indicate a significant slip velocity over the hydrophobic surfaces, increasing with shear rate. The linear dependence of slip length on shear rate assumed by the data fitting procedure appears reasonable and the data closely follow the assumed model. Perhaps more surprising is the presence of a slip length over the hydrophilic surfaces. The necessary adjustment to the prebonding measurements of the channel heights described above was found to be -35 nm for the $h=0.5 \mu\text{m}$ channels and -65 nm for the $h=1 \mu\text{m}$ channels. This discrepancy between the prebonding measurements and the height inferred from the flow measurements remains a source of puzzlement and concern. However, it is consistent with similar measurements using multiple fluids in similar channels fabricated at the same time.²⁰ This consis-

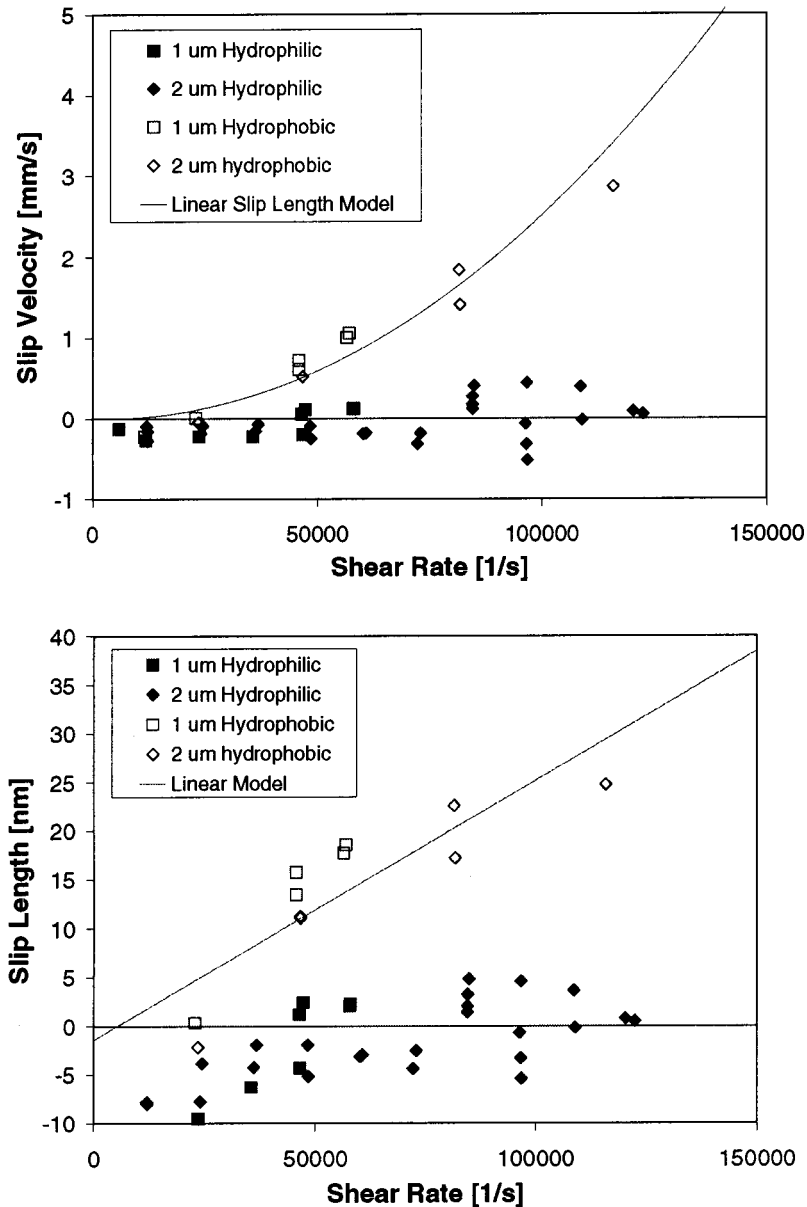


FIG. 4. Slip velocity and associated slip length for pure DI water versus rate of shear. All experimental data from all channels are plotted here. The data analysis described in the text is constrained to minimize the slip velocity over the hydrophilic surface. The slip length dependence for the hydrophobic surface is $\delta = -1.4 + 2.7 \times 10^{-4} \dot{\gamma}$.

tent deviation suggests that the discrepancy might be due to an error incurred during the profilometer measurements, or due to a change in the height induced by the elevated temperatures and pressures experienced during the anodic bonding and RCA-1 cleaning processes. The consistency of all these data, however, leads us to believe that the *in situ* measurements are more reliable and that the subsequent conclusions are valid.

In order to explore the robustness of these results, and the sensitivity to the channel height adjustment, a second strategy of optimization was also performed. In this scenario, we explore the hypothesis that there is no slip over the hydrophilic surface. In order to enforce this constraint, the channel heights were each relaxed from their prebonding baseline such that the rms slip velocity over the hydrophilic surface was minimized. This is a local optimization that is performed independently for each channel using only the hydrophilic flow data from that channel. It does not depend

on data obtained from the other channels. The optimal channel heights that minimized the hydrophilic slip velocities were found to be almost identical to the previous (unconstrained) optimal values of h , although larger in each case by less than 10 nm. Following this step, the slip length dependence over the hydrophobic surfaces, $\delta = A + B \dot{\gamma}$, was determined, as before, by linear regression.

The results of this new analysis are shown in Fig. 4. Several observations are warranted. The change in the values of h between the free optimization of Fig. 3 and the constrained optimization are *very small*—less than 10 nm for each channel—even though the data analysis for the two cases focuses on quite different optimization constraints. This consistency between the two analyses suggests that these values of h are both robust and reliable. It should be noted that the rms error between the model predictions and the experimental measurements of the slip length is slightly lower for the completely unconstrained case in Fig. 3 (3.3

nm) than for the constrained case in Fig. 4 (4.0 nm). Despite the uncertainty allowed by the technique of data analysis, and the unsolved question as to whether there exists slip over the hydrophilic surface, the presence of slip over the hydrophobic surface seems incontrovertible, and no amount of relaxation of the channel height can eliminate the clear distinction between the data from the hydrophilic and hydrophobic surfaces.

The least squares minimization technique does allow for the data to be fit to a very general representation of the slip length and the form chosen here was not based on any theoretical model but solely on the visual appearance of the experimentally derived data. Other model forms were also tested and are described briefly here. A power dependence on shear rate: $\delta = A\dot{\gamma}^B$ was tested²¹ and was found to fit the experimental data slightly better than the linear dependence described above (rms error 2.9 nm), however the exponent of $B \approx 0.5$ seemed somewhat arbitrary and the linear dependence presented here was deemed more plausible. The slip model proposed by Thompson and Troian²² was considered, but not tested since the character of the experimental data for δ indicates, if anything, a concave-down dependence on $\dot{\gamma}$, and shows no sign of the finite shear rate singularity observed by Thompson and Troian. However, the range of the current experimental data does not reach the high shear rates explored in the molecular dynamics simulations of Thompson and Troian. In addition, the flow geometry is somewhat different (a Poiseuille flow in the present case compared with a very small gap Couette flow in the Thompson–Troian computations). For these reasons, comparisons between the two results may not be completely appropriate. Lastly, the Navier slip model may not be the best framework in which to analyze these (and other) data. Other models²³ may prove useful as the experimental database grows.

IV. CONCLUDING REMARKS

In conclusion, the apparent slip effects of water flow in hydrophilic and hydrophobic microchannels have been examined experimentally using precision measurements of flow rate versus pressure drop, and correlating the results to an analytical solution of flow through a channel with a slip velocity at the wall. Some ambiguity in the experimental data is unfortunately present, primarily due to uncertainties in the exact channel height—an uncertainty to which this analysis is particularly sensitive. Different assumptions about the nature of the slip velocity can alter the interpretation of the result. However the fundamental conclusion is clear—that there exists a discernable difference between the boundary condition between water at a hydrophilic and at a hydrophobic surface. The slip length is observed to increase approximately linearly with shear rate, with a value of approximately 30 nm at a shear rate of 10^5 s^{-1} . Other functional dependencies for $\delta(\dot{\gamma})$ might also be supported by the data. Several potential problems that might contaminate these results have been suggested, examined and discarded. The effects of high driving pressure, such as compressibility of the fluid or pressure-dependent viscosity, are not relevant at these relatively low pressures,²⁴ and viscous heating also

is negligible at these flow conditions. Mechanical deformation of the channel walls was also estimated and rejected (the channel is firmly clamped in a steel fixture during testing). Other factors are already known to affect slip, including surface roughness²⁵ and dissolved gases in the working fluid.²⁶ As noted before, the surface roughness fell due to the OTS coating, a fact that, by itself, could be responsible for some of the increased slip behavior. The effects of dissolved gases is of particular concern in the present experiments due to the method by which the water is forced through the microchannels. This concern was alleviated by estimating the time required for nitrogen to dissolve into the water at the free surface and confirming that this time is far longer than the duration of a typical experiment.¹⁴ Second, selected experiments were repeated, with consistent results at elevated pressures. Nevertheless, further testing is planned to test in a more systematic fashion these and other potential sources of inaccuracy. Future work will include the development of a more direct determination of the channel height after bonding (using interferometry), thus removing the ambiguity in the present technique and direct measurement of the surface velocity, using flow visualization through the glass window that forms one of the walls.

ACKNOWLEDGMENTS

This work was supported by DARPA. The authors would like to acknowledge the help of Zhiqiang Cao and Peter Huang, and to thank G. M. Homsy for his constructive comments as this work has evolved.

¹N. Churaev, V. Sobolev, and A. Somov, “Slippage of liquids over lyophobic solid surfaces,” *J. Colloid Interface Sci.* **97**, 574 (1984).

²R. Pit, H. Hervet, and L. Leger, “Direct experimental evidence of slip in hexadecane: Solid interfaces,” *Phys. Rev. Lett.* **85**, 980 (2000).

³E. Ruckenstein and P. Rajora, “On the no-slip boundary condition of hydrodynamics,” *J. Colloid Interface Sci.* **96**, 488 (1983).

⁴E. Schnell, “Slippage of water over nonwetable surfaces,” *J. Appl. Phys.* **27**, 1149 (1956).

⁵D. Tretheway and C. Meinhart, “Apparent fluid slip at hydrophobic microchannel walls,” *Phys. Fluids* **14**, L9 (2002).

⁶K. Watanabe, Y. Udagawa, and H. Mizunuma, “Slip of Newtonian fluids at slip boundary,” *J. Fluid Mech.* **381**, 225 (1999).

⁷Y. Zhu and S. Granick, “Rate-dependent slip of Newtonian liquid at smooth surfaces,” *Phys. Rev. Lett.* **87**, 096105 (2001).

⁸V. S. Craig, C. Neto, and D. R. Williams, “Shear-dependent boundary slip in an aqueous Newtonian liquid,” *Phys. Rev. Lett.* **87**, 054504 (2001).

⁹E. B. Arkilic, M. A. Schmidt, and K. S. Breuer, “Gaseous slip flow in long microchannels,” *J. Microelectromech. Syst.* **6**, 167 (1997).

¹⁰E. Arkilic, M. Schmidt, and K. Breuer, “Slip flows and tangential momentum accommodation in micromachined channels,” *J. Fluid Mech.* **437**, 29 (2001).

¹¹B. Ziaie, J. Von Arx, M. Dokmeci, and K. Najafi, “A hermetic glass-silicon micropackage with high-density on-chip feedthroughs for sensors and actuators,” *J. Microelectromech. Syst.* **5**, 166 (1996).

¹²W. Ko, J. Suminto, and G. Yeh, “Bonding techniques for microsensors,” in *Micromachining and Micropackaging of Transducers* (Elsevier, New York, 1985), p. 41.

¹³G. Wallis and D. Pomerantz, “Field assisted glass–metal sealing,” *J. Appl. Phys.* **40**, 3946 (1969).

¹⁴K. J. A. Westin, C.-H. Choi, and K. S. Breuer, “A novel system for measuring liquid flow rates with nanoliter per minute resolution,” *Exp. Fluids* **34**, 635 (2003).

¹⁵H. Okorn-Schmidt, “Characterization of silicon surface preparation processes for advanced gate dielectrics,” *IBM J. Res. Dev.* **43**, 351 (1999).

¹⁶A. Richter, “*In situ* and interrupted growth studies of self-assembled mono-

- layers using x-ray reflectivity," Ph.D. thesis, Northwestern University, 2000.
- ¹⁷S. Wasserman, Y.-T. Tao, and G. Whitesides, "Structure and reactivity of alkylsiloxane monolayers formed by reaction of alkyltrichlorosilanes on silicon substrates," *Langmuir* **5**, 1074 (1989).
- ¹⁸J. Brzoska, N. Shahidzadeh, and F. Rondelez, "Evidence of a transition temperature for the optimum deposition of grafted monolayer coatings," *Nature (London)* **360**, 719 (1992).
- ¹⁹M. Goldmann, J. V. Davidovits, V. Pho, and P. Silberzan, "Temperature influence on the formation of silanized monolayers on silica: An atomic force microscopy study," *Surf. Sci.* **352**, 369 (1996).
- ²⁰K. J. A. Westin, K. S. Breuer, C.-H. Choi, P. Huang, Z. Cao, B. Caswell, P. D. Richardson, and M. Sibalukin, "Liquid transport properties in sub-micron channel flows," in *Proceedings of IMECE2001, 2001 International Mechanical Engineering Conference and Exposition*, New York (ASME, New York, 2001).
- ²¹C.-H. Choi, K. J. A. Westin, and K. S. Breuer, "To slip or not to slip: Water flows in hydrophilic and hydrophobic microchannels," in *Proceedings of IMECE2002, 2002 International Mechanical Engineering Conference and Exposition*, New Orleans, LA (ASME, New York, 2002), Paper No. 2003-33707.
- ²²P. Thompson and S. Troian, "A general boundary condition for liquid flow at solid surfaces," *Nature (London)* **389**, 360 (1997).
- ²³H. Spikes and S. Granick, "Equation for slip of simple liquids at smooth solid surfaces," *Langmuir* **2003**, 5065 (2003).
- ²⁴P. Bridgman, *The Physics of High Pressure* (G. Bell and Sons, London, 1949).
- ²⁵Y. Zhu and S. Granick, "Limits of the hydrodynamics no-slip boundary condition," *Phys. Rev. Lett.* **88**, 106102 (2002).
- ²⁶S. Granick, Y. Zhu, and H. Lee, "Slippery questions about complex fluids flowing past solids," *Nat. Mater.* **2**, 221 (2003).